

CHOOSING THE MESH-INDEPENDENT SUB-GRID DRAG COEFFICIENT MODEL

Bona LU^{a,b}, Wei WANG^{a,*}, Jinghai LI^{a,*}

^aState Key Laboratory of Multi-phase Complex System, Institute of Process Engineering, Chinese Academy of Sciences, PO Box 353, Beijing, 100190, China

^bGraduate University of Chinese Academy of Sciences, Beijing 100049, China

ABSTRACT

This work aims to investigate whether it is suitable for simulating a circulating fluidized bed (CFB) riser to apply the fine-grid simulation of the two-fluid model (TFM) with a classic drag coefficient? Our tentative answer is NO, merely grid refining is not sufficient to get a correct prediction of the two-phase flow behaviour. Furthermore, we attempt to search for a mesh-independent sub-grid drag model by applying a multiscale method. To these ends, we arrange the following numerical experiments. Firstly, the simulations with a classic drag model (model G for short) (Gidaspow, 1986) and a multiscale drag model (model M for short) (Wang and Li, 2007; Lu et al., 2009) are performed in a doubly-periodic domain whose size is comparative to the grid size used in coarse-grid simulations for riser flows, where different grid resolutions are prescribed to investigate the effect of grid size. As no global acceleration exists in a periodic domain, the total drag force exerted on particles within the domain relates to the effective gravity as $\beta = \varepsilon_g \varepsilon_s (\rho_p - \rho_g) g / u_{slip}$, and then higher slip velocity means lower drag coefficient in a periodic domain. This is the basis of the evaluation of the grid size effects. Secondly, the simulations with both drag models are performed for a CFB riser with the mesh that is fine enough to represent the real solution of TFM. The effect of the particle properties is especially studied by including two types of particle, i.e. FCC particle belonging to Geldart A and glass beads belonging to Geldart B in classification (Geldart, 1973).

Fig.1 compares these two drag models in terms of the heterogeneity index, which is calculated by $H_D = \beta / \beta_0$, where β_0 corresponds to the standard Wen and Yu drag coefficient (Wen and Yu, 1966) and β corresponds to the drag coefficient of the compared drag models. For Model M, the drag coefficient is lower than the standard within most of the range except near the two ends of the voidage spectrum corresponding to the packed state and the extremely dilute flow, respectively.

For Geldart A particles, it is found in Fig. 2a that the averaged slip velocity for the case of model G varies with the grid size and approaches an asymptotic solution when the grid size is around 10 times the particle diameter, and thereon the dimensionless slip velocity is about 2. For model M, the dimensionless slip velocity is insensitive to the grid refining and its value remains almost unchanged around 5. However, the overall appearance of the snapshots in Fig. 2a mainly depends on the mesh resolution instead of the choice of drag models. Applications of these drag models in riser simulations show that the model G fails to capture the characteristic S-shaped axial voidage profile even using high grid resolution (shown in Fig. 3a), while the axial voidage profile predicted by model M agrees well with the experimental data.

For Geldart B particles, as shown in Fig. 2b, both drag models predict slip velocities which are almost independent of the mesh over the whole range of grid size, though their values differ for each model. For the case of model G, the predicted slip velocity is around the terminal velocity of a single particle (u_T). That means: TFM can probably be used to predict a riser with Geldart B particles even with coarse grids and the classic drag models. However, the quantitative validation needs more verification for these two drag models. As what we have compared in Fig. 3b, the axial pressure profile still differs for these two drag models though the discrepancy may be not as large as the case for Geldart A particles.

In summary, the effects of the sub-grid structure always exist for the gas-solid two-phase flow, while the role of the effects differs for different particles. The fine-grid simulation is not enough for the simulation of a gas-solid riser flow. The sub-grid modelling with multiscale methods is expected as a new paradigm for CFB simulations.

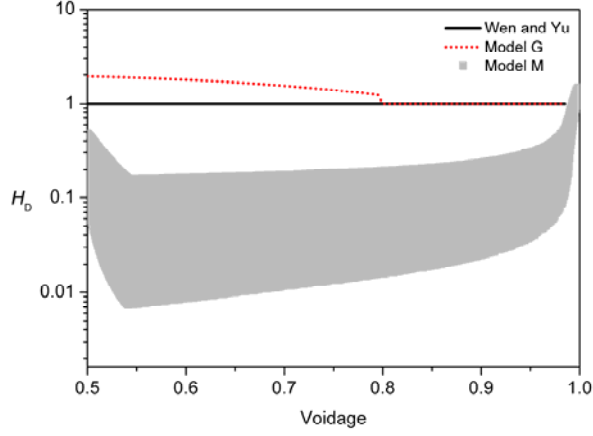


Fig. 1. Comparison of drag models in terms of the heterogeneity index as a function of voidage (FCC/air system: $\rho_p=930 \text{ kg}\cdot\text{m}^{-3}$, $d_p=54 \text{ }\mu\text{m}$, $U_g=1.52 \text{ m}\cdot\text{s}^{-1}$, $G_s=14.3 \text{ kg}\cdot\text{m}^{-2}\cdot\text{s}^{-1}$, $\epsilon_{mf}=0.4$, $\epsilon_{max}=0.9997$), $Re_p \in [0.001, 33]$ for model M, $Re_p=5$ for model G

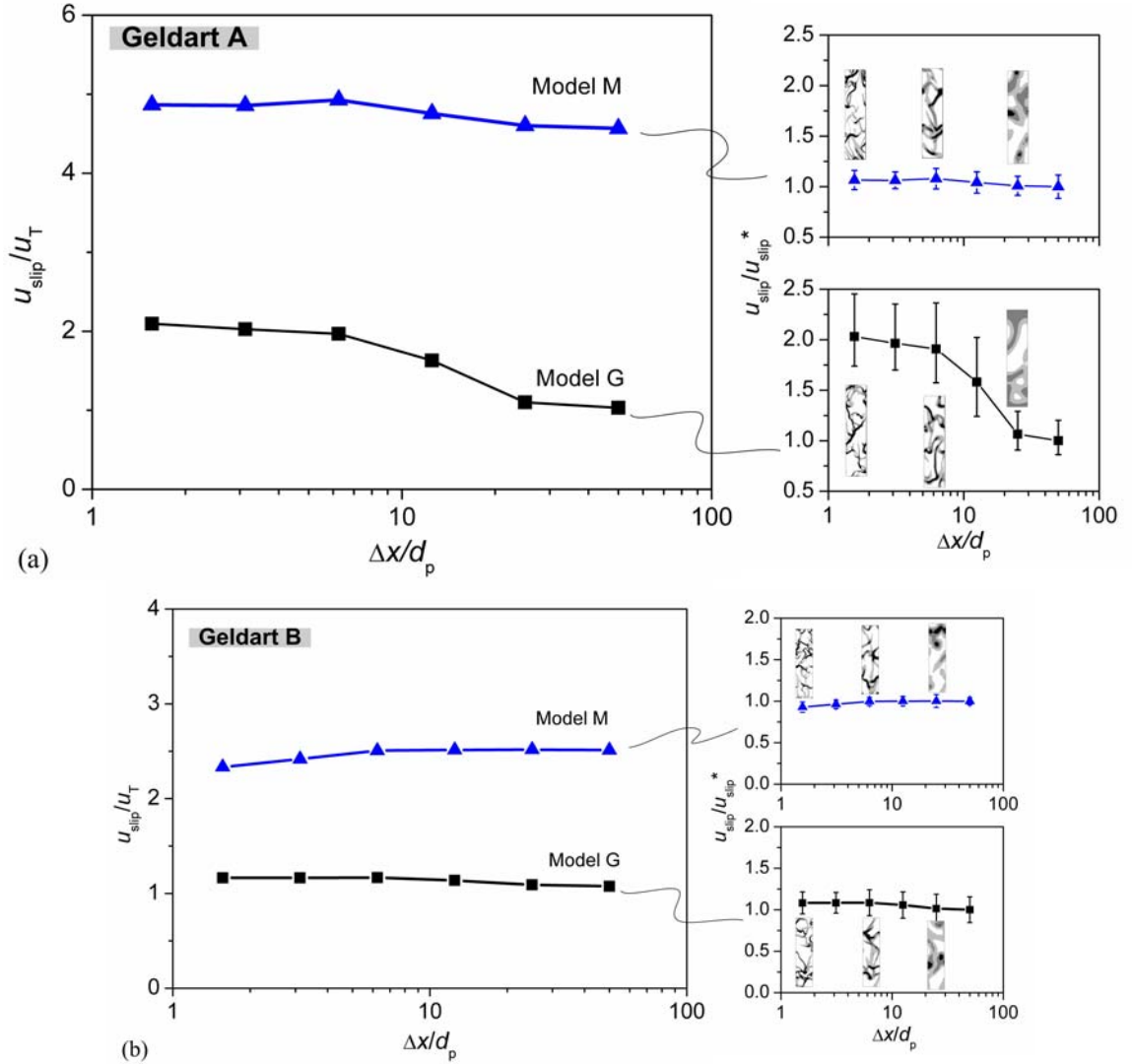
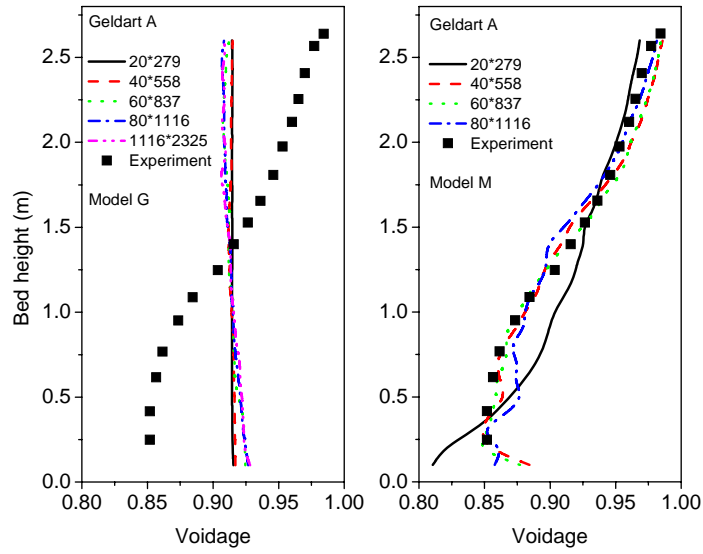
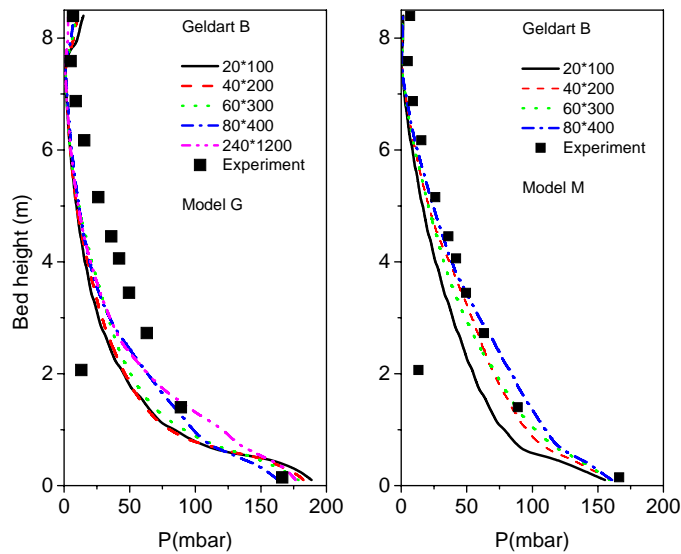


Fig. 2. Effects of grid size (Δx) on the time-averaged axial slip velocity (u_{slip}) with snapshots of solids distribution, u_{slip}^* is the time-averaged slip velocity at $\Delta x/d_p=50$ in periodic domain simulations, average solids concentration is 0.05 : (a) with Geldart A particles ($\rho_p=1500 \text{ kg}\cdot\text{m}^{-3}$, $d_p=75 \mu\text{m}$, $\epsilon_{mf}=0.4$, domain size= $1.5 \times 6 \text{ cm}^2$); (b) with Geldart B particles ($\rho_p=2500 \text{ kg}\cdot\text{m}^{-3}$, $d_p=300 \mu\text{m}$, $\epsilon_{mf}=0.4$, domain size= $6 \times 24 \text{ cm}^2$)



(a)



(b)

Fig. 3. Axial profiles of voidage and pressure with different grid resolutions, simulations are performed with circulating mode similar to Lu et al.(2009): (a) axial voidage profiles for riser flows with Geldart A particles ($H=2.79$ m, $I.D.=0.05$ m, $\rho_p=1000$ $\text{kg}\cdot\text{m}^{-3}$, $d_p=60$ μm , $U_g=1.17$ $\text{m}\cdot\text{s}^{-1}$, $G_s=11.7$ $\text{kg}\cdot\text{m}^{-2}\cdot\text{s}^{-1}$, average concentration is 0.086), the experiment is cited from Horio et al.(1988); (b) axial voidage profiles for riser flows with Geldart B particles ($H=8.5$ m, $I.D.=0.411$ m, $\rho_p=2500$ $\text{kg}\cdot\text{m}^{-3}$, $d_p=300$ μm , $U_g=7.76$ $\text{m}\cdot\text{s}^{-1}$, $G_s=151.6$ $\text{kg}\cdot\text{m}^{-2}\cdot\text{s}^{-1}$, averaged concentration is 0.084), the experimental data are obtained from ETH-CFB database (Herbert and Reh, 1999)

REFERENCES

- D. GIDASPOW, (1986), "Hydrodynamics of fluidization and heat transfer: supercomputer modeling", *Applied Mechanics Reviews* 39, 1-23.
- W. WANG AND J. LI, (2007), "Simulation of gas-solid two-phase flow by a multi-scale CFD approach-extension of EMMS model to the sub-grid level." *Chemical Engineering Science* 62, 208-231.
- B. LU ET AL., (2009), "Searching for a mesh-independent sub-grid model for CFD simulation of gas-solid riser flows", *Chemical Engineering Science* 64 (15), 3437-3447.
- D. GELDART, (1973), "Types of gas fluidization", *Powder Technology* 7, 185-195.

C. Y. WEN AND Y. H. YU, (1966), "Mechanics of fluidization", *Chemical Engineering Symposium Series* 62 (62), 100-111.

M. HORIO ET AL., 1988. *Solid distribution and movement in circulating fluidized beds. Circulating Fluidized Bed Technology II*, Pergamon.

P. HERBERT AND L. REH, 1999. *ETH-CFB measurement database: General description and operations manual: 1-29.*